Spatio-temporal intensity dynamics of passively mode-locked fiber laser

Dmitry V. Churkin[a,b,c] and Srikanth Sugavanam[a]

[a]Aston Institute of Photonic Technologies, Aston University, Birmingham B4 7ET, United Kingdom
[b]Novosibirsk State University, Novosibirsk 630090, Russia
[c]Institute of Computational Technologies, Siberian Branch of the Russian Academy of Sciences, Novosibirsk 630090, Russia

ABSTRACT

We present recent results on measurements of intensity spatio-temporal dynamics in passively mode-locked fibre laser. We experimentally uncover distinct, dynamic and stable spatio-temporal generation regimes of various stochasticity and periodicity properties in though-to-be unstable laser. We present a method to distinguish various types of generated coherent structures, including rogue and shock waves, within the radiation by means of introducing of intensity ACF evolution map. We also discuss how the spectral dynamics could be measured in fiber lasers generating irregular train of pulses of quasi-CW generation via combination of heterodyning and intensity spatio-temporal measurement concept.

Keywords: fibre lasers, spatio-temporal dynamics, real-time measurements, coherent structures, rogue waves

1. INTRODUCTION

Conventionally, lasers are the epitome of stable optical output, but as the industrial development pushes for shorter pulses and higher energies, non-linear interaction of light with its medium could result in complex generation regimes. This is in particular the case of long fibre lasers which are well known for their complex non-linear regimes 1–3. The regimes could vary substantially: noise-like pulses 4, double-scale femto-/pico-second noisy pulses 5, generation of soliton rains 6,7, soliton molecules 8, dark solitons 9. In addition, complex processes of their interaction like soliton explosions 10, 11 and rogue wave generation 12–15 have also been observed. In some cases, even optical turbulence in generation of mode-locked lasers may be observed 16–20. Understanding and mastering this variety of non-linear generation regimes may lead to development of new laser types with new features and better performance.

Sometimes, seemingly chaotic output in long fibre cavities could limit the performance achievable in laser systems. Indeed, in practical applications, experimentalists usually tend to avoid such complex regimes because of challenges posed by their irregularity. However, such highly non-linear generation regimes could be understood more in a bid to discover new modalities and develop better lasers.

In the present manuscript, we describe various spatio-temporal generation regimes in passively mode-locked fibre laser. We use the concept of spatio-temporal generation regimes described in recent article 21.

2. SPATIO-TEMPORAL GENERATION REGIMES OF PASSIVELY MODE-LOCKED FIBRE LASER

We operate a one-kilometre-long partially mode-locked laser in a regime of noise-like pulses, Fig. 1. Such temporal dynamics usually indicates that a laser is simply unstable. However, as the laser radiation is trapped in the cavity making round trips within, long-range temporal correlations do exist at time intervals being 56 orders of magnitude larger than the typical intensity fluctuation time within the pulse. Measuring consecutive

Further author information: (Send correspondence to D.V.C.)
D.V.C.: E-mail: d.churkin@aston.ac.uk

Real-time Measurements, Rogue Events, and Emerging Applications, edited by Bahram Jalali, Sergei K. Turitsyn, Daniel R. Solli, John M. Dudley, Proc. of SPIE Vol. 9732, 97320I · © 2016 SPIE · CCC code: 0277-786X/16/$18 · doi: 10.1117/12.2211762

snapshots of the radiation circulating within the cavity, it is found that the laser behaviour exceeds mundane one-dimensional intensity-time dependence, oscillating in a dynamic, albeit complex spatio-temporal regeneration regime [2]. This regime is stable over slow evolution coordinate in the sense that it reproduces itself, and laser does not hop from one regime to another. Additionally, what was earlier considered noisy, purely chaotic radiation conceals prominent coherent features surrounded by a background and reproduced over many round trips, similar to waves riding the ocean surface.

As a test-bed system for analysis of stochasticity and periodicity in passively mode-locked fibre lasers, we adopted a 1-km long NPE mode-locked normal dispersion ring cavity fibre laser, Fig.1. The particular design of the laser cavity is not important for considered problems of characterization of spatio-temporal intensity dynamics of the laser output. However, we chose a relatively long cavity (1 km in our case) to reduce laser stability and have access to a variety of complex regimes. It is known that in long passively mode-locked lasers a variety of regimes could be observed 22. Output from the laser is obtained from one arm of a polarization beam splitter. This output is sent through a coupler configuration to allow simultaneous measurement of power, optical spectra and intensity dynamics. The spectral resolution of the optical spectrum analyzer was 20 pm. A 25 GHz oscilloscope, with a sampling rate of 80 GS/s and a total signal length of 512 Mpts was used to measure the long term intensity dynamics. The sampling rate of the scope was adjustable, allowing us to observe temporal dynamics over longer time scales. The obtained time signals were processed using the software MATLAB. MATLAB was chosen for this application as it is particularly well suited for matrix based algorithms.

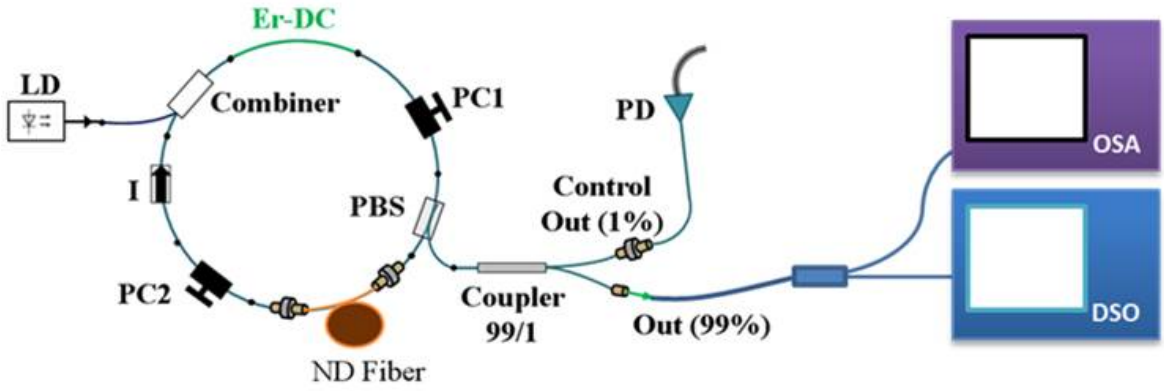

Figure 1. The passively mode-locked fibre laser under investigation. Er-DC Erbium doped fiber gain medium, LD Laser diode (pump source for Er-DC), PC1,PC2 Polarization controllers, PBS polarization beam splitter, ND 1 km Normal dispersion fiber ($D = -44$ ps/nm/km), PD Photo detector based power meter, OSA Optical spectrum analyzer, DSO Digital storage oscilloscope.

The laser generates broad stochastically filled pulses, and despite being mode-locked and generating a well-resolved pulse train with fairly stable inter-pulse separation, it may produce pulses of substantially different shape at different moments in time, as the measured intensity dynamics I(t) reveals, Fig. 2(a-d). The experimental challenge here is to decide whether these radically differing temporal profiles belong to the same pulse in the cavity under the influence of some complex non-linear processes leading to strong pulse re-shaping or the laser just hops from one generation regime to another one during its operation and thus can not be considered stable.

To answer this question, we measure very long intensity time traces in real-time, $I(t)$, and then construct from such traces the spatio-temporal intensity dynamics, $I(t, z)$, which reveal both dynamics over fast time t and slow evolution propagation coordinate z measured in our case as a number of cavity round-trips. The measured spatio-temporal dynamics immediately reveals internal periodicity of the pulse evolution over the slow evolution coordinate , despite its stochastic nature over fast time t, Fig.2(e). The pulse exhibits a complex dynamics over the slow evolution coordinate with a typical evolution time equivalent to hundreds of round-trips. The pulse has a sustaining shock-type trailing edge and smooth leading front.

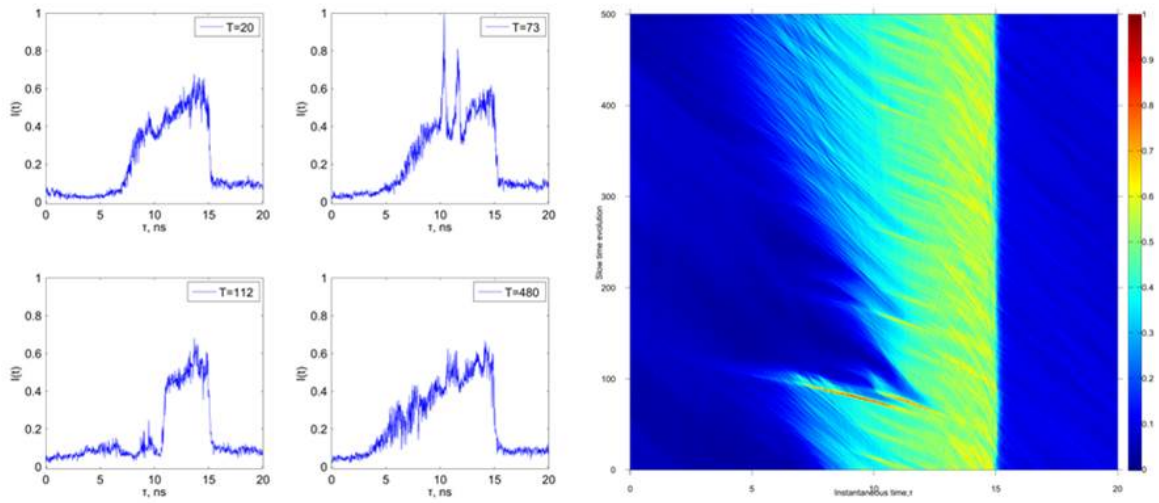

Figure 2. Temporal and spatio-temporal intensity dynamics of a long passively mode-locked fibre laser. (a-d) Experimentally measured pulse shapes at different moments of time showing stochastic nature of the laser regime. (e) Corresponding spatio-temporal intensity dynamics revealing internal periodicity in the stochastic laser radiation. Intensity is colour-coded on a linear scale.

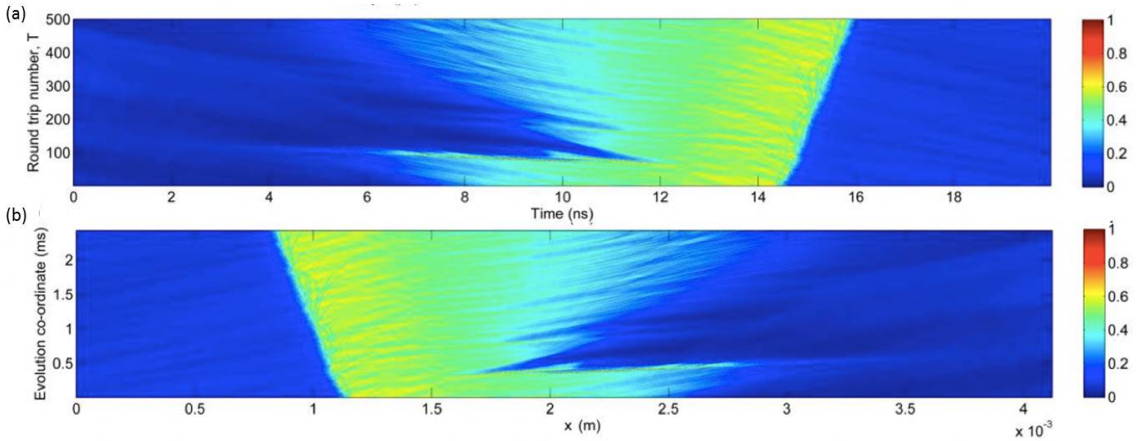

Figure 3. Temporal and spatial coordinates on intensity spatio-temporal dynamics. (a) Dynamics $I(t, z)$ in coordinates: fast time t and evolution longitudinal coordianate, z, measured as a number of cavity-round trips. (b) Dynamics $I(x, T)$ in coordinates: space, x, and slow evolution time, T.

Let us clarify how we treat spatial and temporal coordinates in the obtained intensity spatio-temporal dynamics. This could be done in two complementary ways, Fig. 3. In the first way, the initial temporal dynamics, $I(t)$ is represented as a intensity dynamics over fast time t which physically corresponds to the initial data from the photodiode. The given pattern of intensity dynamics $I(t)$ slowly evolves over the slow evolution longitudinal coordinate, z, which is naturally measured in our approach as a number N of laser cavity round-trips and could be represented as such a number or as a corresponding discrete spatial coordinate $z = N \cdot L$, where L is the cavity length. As a result, the laser is characterized by its spatio-temporal dynamics $I(t, z)$, Fig.3(a). Let's us recall the corresponding notations in nonlinear Schrodinger equation, in which t corresponds to a term with second derivative, while z corresponds to a term with a first derivative in NLSE. The complementary way is to make a transformation t to $t - x/c$, where c is the speed of light in the media, x is the spatial coordinate. In other words, an instant photo in the laser intensity is made, so the laser pulse occupies some space over fiber over its longitudinal coordinate. In this way one have a spatial distribution of pulse's intensity over space, $I(x)$.

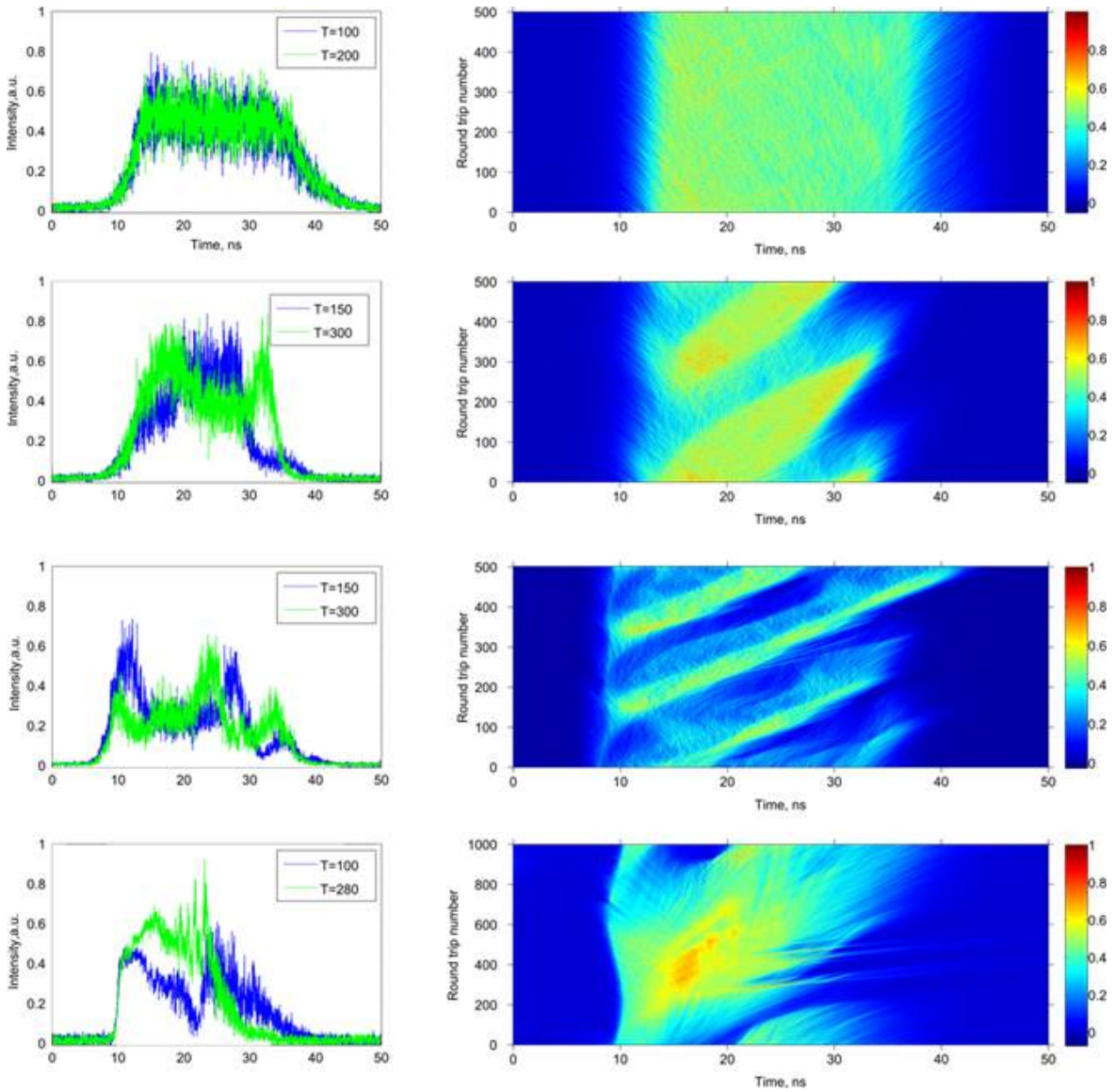

Figure 4. Different types of spatio-temporal regimes with different periodicity properties. (a) A stochastic pulse stable over the slow evolution coordinage. (b, c) Examples of regimes having well-pronounced periodicity over the evolution coordinate. (d) A stochastic pulse localized both over fast time and slow evolution coordinate. Right column in all panels is spatio-temporal intensity dynamics. Left column shows the corresponding pulse profiles measured at evolution time T indicated by dotted lines in spatio-temporal intensity diagrams.

Then one traces how this given spatial distribution of intensity, $I(x)$, evolves over slow evolution time T (first derivative in NLSE). Slow evolution time T is measured again as a number of cavity round-trips, $T = N \cdot T_{rt}$, where T_{rt} is cavity round-trip time. The resulted spatio-temporal dynamics, $I(x, T)$ has a mirror symmetry over the X axis comparing with spatio-temporal dynamics $I(t, z)$, Fig.3(b).

Further on, we set the laser to generate different types of stochastic pulses with different spatio-temporal structure, Fig.4(a-d). Although the stochastic pulse shapes appear very similar in all presented regimes (see Fig.4, left column), these regimes are very different in their periodicity properties over the slow evolution time coordinate. They vary from one featuring completely homogenous evolution over round-trips, Fig. 4(a), to regimes with well-pronounced evolution periodicity, Fig.4(b,c), and, finally, to those where the pulse tends to be

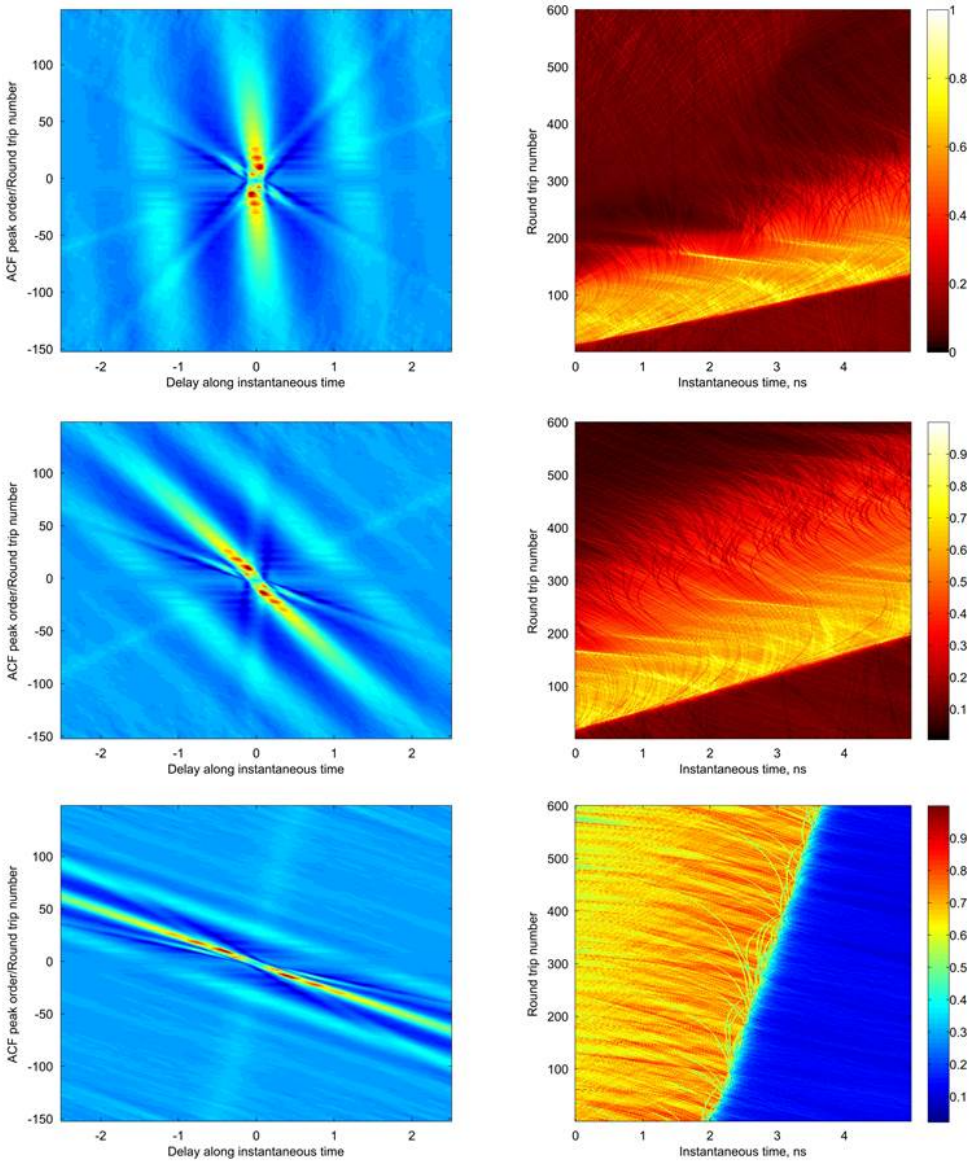

Figure 5. Intensity auto-correletaion function map (left column) and intensity spatio-temporal dynamics plotted in corresponding reference frame (right column). Different structures within the radiation having different group velocities shift over fast time t while evolving over slow evolution coordinate T, resulting in straight lines on the ACF evolution dynamics. Different details of dark solitons interaction with stochastic pulse are visible in different co-moving reference frames (shown on different rows).

localised over both the spatial coordinate and evolution coordinate, Fig. 4(d). In all cases, except Fig. 4(a), the pulse shape is subject to pronounced modification over the course of its evolution (left column in Fig. 4). In this way, the laser operates not in the distinct temporal regimes, but in the given spatio-temporal regime, which could be dynamic (the temporal profile of the pulse $I(t)$ is changed over evolution over slow evolution coordinate), but is stable (the regime reproduces itself over slow evolution coordinate).

Different types of coherent and dissipative structures may be embedded in stochastic radiation. To reveal constituents of the studied radiation, we utilise an autocorrelation analysis. We measure the intensity autocorrelation function (ACF) defined as $K(\tau) =< I(t) \cdot I(t+\tau) >_t$ directly with a real-time oscilloscope to have access

to large detuning times τ, which is crucial for identification of coherent structures within stochastic radiation. The intensity autocorrelation function measured over a large number of round-trips has a comb-like structure comprising a series of peaks separated by T_{rt} because the intra-cavity radiation evolves quasi-periodically in the laser cavity (with an approximate period equal to round-trip time T_{rt}. Zero-order ACF peak resulting from two overlaid pulse train replicas appears at $\tau = 0$ could have different time scales. In our case a narrow autocorrelation peak (of about 100-ps width) is sitting on top of a wider background (about 10 ns wide). The narrow ACF peak corresponds to the typical time scale of intensity fluctuations defining the stochastic nature of the pulse, while the broad pedestal reflects the average width of the noise-like pulse. Note that although we observe a double-scale ACF, it is different from the one previously studied in mode-locked lasers 4,5. Indeed, in our case of partial mode locking, stochastic pulses are much broader, so the smaller scale in the zero-order ACF for broad pulses is of similar temporal width as the wide pedestal of more stable pulses in papers 4, 5.

Each scale of the zero-order ACF peak means that there should be some typical structures of the corresponding temporal width within the total radiation. However, if different types of temporal structures have similar temporal width, they will be mixed up within the same scale of the zero-order ACF peak, becoming unresolvable there. Real-time measurements of intensity ACF over time delays τ up to hundreds of round-trip times T_{rt} with an oscilloscope allow us to tell apart different types of radiation components even if they are of similar temporal width. To do that, we focus on the N-th order ACF peak located at time delay $\tau_N = N \cdot T_{rt}$. The N-th order ACF peak appears as a result of convolution of the intensity pattern with its replica shifted by N cavity round-trips (i.e. the same intensity pattern measured N cavity round-trips later). The radiation partials of different types may also have different group velocities resulting in different time needed for the studied structure to make a round-trip over the cavity. Thus, different structures having different group velocities may contribute to different sub-peaks superimposed on the main N-th order ACF peak. Indeed, higher-order intensity ACF peaks reveal certain signs of additional small amplitude peaks shifted off the centre of the main peak.

Similar to time domain, one-dimensional representation of intensity ACF does not allow us to identify different structures rigorously. This is first of all caused by extremely small typical group velocity differences between different types of coherent structures and dispersive waves which could be as small as $10^4 - 10^5$. Another obstacle is a small amount of energy in those structures compared to the total energy in the radiation leading to tiny, poorly resolved features in the N-th order ACF peak and making any quantitative analysis impossible. To overcome this problem, we build a two-dimensional intensity ACF evolution map by plotting the ACF signal over time detuning τ_1 and number N. Here $N = 0, \pm1, \pm2$, etc. is the order of the ACF peak effectively representing the number of round-trips and time detuning $\tau_1 = \tau - N \cdot T_{rt}$ so that $\mid \tau_1 \mid < T_{rt}/2$. The ACF evolution map is shown in left column of Fig. 5.

In general, any temporal structure with a constant group velocity different from that of the co-moving reference frame (used in the definition of T_{rt}) will give a straight slanted line on the ACF evolution map. As a result, we find a number of small satellite auto-correlation peaks, whose position depends linearly on the order of correlation peaks. This approach can be used for characterisation of coherent structures with varying parameters that may be overlooked by other techniques when such structures are embedded into the stochastic radiation background. Different peaks correspond to structures of distinct types. The presence of different structures means, in particular, that the auto-correlation function in its zero-order has actually multiple overlapping scales. By measuring the angle of each satellite line, the group velocity difference of each structure may be determined to precision as high as $10^5 10^6$ and further used to adjust the value of T_{rt} and to finally plot the spatio-temporal intensity dynamics, $I(t, z)$, in a co-moving reference frame selected so as to almost immobilise the structures of interest and, therefore, make them directly detectable. The resulted spatio-temporal dynamics plotted in different co-moving reference frames having a speed derived as described above are shown of Fig. 5, right column.

The spatio-temporal dynamics presented in different co-moving reference frames highlight dynamics of coherent structures in the radiation. Dark traces clearly visible on Fig. 5, right column are dark and grey solitons generation on the interpulse laminar background 9. In 23, it was numerically found that dark/grey solitons are generated at the initial stage of radiation build-up in passively mode-locked fibre lasers, although they eventually decay. Here we experimentally observe generation of dark/grey solitons in stable generation regime.

3. DISCUSSION

Simple measurements provide a fresh insight into the world of laser dynamics and present a very simple, elegant key to understanding it. Indeed, spatio-temporal generation regimes are found in various systems: as laminar and turbulent states in quasi-CW fibre lasers 9, as topological solitons with controlled phase information for next-generation coherent communication systems 24. Similar measurements could help to reveal hidden periodicity in the cavity-less lasers, such as random distributed feedback fibre lasers 25,26. Such lasers share many generation properties with conventional Raman fibre laser including possibility to polarized output 27, high-efficiency generation,[28] multi-wavelength 29 and tunable 30 generation. What is more important temporal dynamics of such lasers is defined as well by multiple turbulent like four-wave mixing processes 31, 32 which make their temporal radiation looking almost stochastic. However, as turbulent regimes of quasi-CW fibre lasers are subject to a great diversity 20, 33, one could expect similar diversity in regimes of random fibre lasers. Recent demonstrations of generation of noise-like pulses in random fibre lasers 34 could be a first step to further extensions of possibilities of such lasers. Similar methodology proved to be highly efficient in investigating of dynamics of different types of quasi-CW lasers, e.g. Raman fibre lasers in which differnet types of turbulent generation have been found 19, 35.

Not limited to any type of a laser, spatio-temporal dynamics could be measured in any dynamical system exhibiting some form of periodicity, which is isolated in spatio-temporal dynamics, for example, it proved to be effient in studies of temporal cavity solitons 36, 37. Furthermore, much more experimental insight could be gained if real-time spectral measurements, for example via dispersive Fourier transform 38. Recent examples of studies of such spectral evolution includes investigation of soliton explosions 11, 39 or rogue waves in normal dispersion fibre laser 40. Another possibility to record real-time spectral dynamics includes PASTA technique 41 which could be potentially combined with real-time intensity spatio-temporal dynamics measurements. Finally, technical limitations imposed by limited bandwidth of real-time oscilloscope could be partially overcome by new emerging techniques like an asynchronous optical sampling technique used in 17, 42.

ACKNOWLEDGMENTS

Authors acknowledge the support of the ERC project UltraLaser, Russian Ministry of Science and Education (agreement 14.584.21.0014), Russian Foundation for Basic Research (projects 16-32-60153, 15-02-07925). Authors thanks N. Tarasov for important contribution to this work.

REFERENCES

[1] Grelu, P. and Akhmediev, N., "Dissipative solitons for mode-locked lasers," *Nat Photon* **6**, 84–92 (Feb. 2012).

[2] Runge, A. F. J., Aguergaray, C., Broderick, N. G. R., and Erkintalo, M., "Coherence and shot-to-shot spectral fluctuations in noise-like ultrafast fiber lasers," *Opt. Lett.* **38**, 4327–4330 (Nov 2013).

[3] Kobtsev, S. and Smirnov, S., "Fiber lasers mode-locked due to nonlinear polarization evolution: golden mean of cavity length," *Laser Physics* **21**(2), 272–276 (2011).

[4] Horowitz, M., Barad, Y., and Silberberg, Y., "Noiselike pulses with a broadband spectrum generated from an erbium-doped fiber laser," *Optics letters* **22**(11), 799–801 (1997).

[5] Kobtsev, S., Kukarin, S., Smirnov, S., Turitsyn, S., and Latkin, A., "Generation of double-scale femto/pico-second optical lumps in mode-locked fiber lasers," *Optics Express* **17**(23), 20707–20713 (2009).

[6] Chouli, S. and Grelu, P., "Rains of solitons in a fiber laser," *Opt. Express* **17**, 11776–11781 (Jul 2009).

[7] Chouli, S. and Grelu, P., "Soliton rains in a fiber laser: An experimental study," *Phys. Rev. A* **81**, 063829 (Jun 2010).

[8] Stratmann, M., Pagel, T., and Mitschke, F., "Experimental observation of temporal soliton molecules," *Phys. Rev. Lett.* **95**, 143902 (Sep 2005).

[9] Turitsyna, E., Smirnov, S., Sugavanam, S., Tarasov, N., Shu, X., Babin, S., Podivilov, E., Churkin, D., Falkovich, G., and Turitsyn, S., "The laminar-turbulent transition in a fibre laser," *Nature Photonics* **7**(10), 783–786 (2013).

[10] Cundiff, S. T., Soto-Crespo, J. M., and Akhmediev, N., "Experimental evidence for soliton explosions," *Phys. Rev. Lett.* **88**, 073903 (Feb 2002).

[11] Runge, A. F. J., Broderick, N. G. R., and Erkintalo, M., "Observation of soliton explosions in a passively mode-locked fiber laser," *Optica* **2**, 36–39 (Jan 2015).

[12] Lecaplain, C., Grelu, P., Soto-Crespo, J. M., and Akhmediev, N., "Dissipative rogue waves generated by chaotic pulse bunching in a mode-locked laser," *Phys. Rev. Lett.* **108**, 233901 (Jun 2012).

[13] Runge, A. F. J., Aguergaray, C., Broderick, N. G. R., and Erkintalo, M., "Raman rogue waves in a partially mode-locked fiber laser," *Opt. Lett.* **39**, 319–322 (Jan 2014).

[14] Lecaplain, C. and Grelu, P., "Rogue waves among noiselike-pulse laser emission: An experimental investigation," *Phys. Rev. A* **90**, 013805 (Jul 2014).

[15] Dudley, J. M., Dias, F., Erkintalo, M., and Genty, G., "Instabilities, breathers and rogue waves in optics," *Nat Photon* **8**, 755–764 (Oct. 2014).

[16] Babin, S. A., Churkin, D. V., Ismagulov, A. E., Kablukov, S. I., and Podivilov, E. V., "Four-wave-mixing-induced turbulent spectral broadening in a long raman fiber laser," *J. Opt. Soc. Am. B* **24**, 1729–1738 (Aug 2007).

[17] Walczak, P., Randoux, S., and Suret, P., "Statistics of a turbulent raman fiber laser," *Optics Letters* **40**(13), 3101–3104 (2015).

[18] Smirnov, S. V., Tarasov, N., and Churkin, D. V., "Radiation build-up in laminar and turbulent regimes in quasi-cw raman fiber laser," *Optics express* **23**(21), 27606–27611 (2015).

[19] Wabnitz, S., "Optical turbulence in fiber lasers," *Opt. Lett.* **39**, 1362–1365 (Mar 2014).

[20] Sugavanam, S., Tarasov, N., Wabnitz, S., and Churkin, D. V., "Ginzburg-landau turbulence in quasi-cw raman fiber lasers," *Laser & Photonics Reviews* **9**(6), L35L39 (2015).

[21] Churkin, D. V., Sugavanam, S., Tarasov, N., Khorev, S., Smirnov, S. V., Kobtsev, S. M., and Turitsyn, S. K., "Stochasticity, periodicity and localized light structures in partially mode-locked fibre lasers," *Nature Communications* **6**, – (May 2015).

[22] Smirnov, S., Kobtsev, S., Kukarin, S., and Ivanenko, A., "Three key regimes of single pulse generation per round trip of all-normal-dispersion fiber lasers mode-locked with nonlinear polarization rotation," *Opt. Express* **20**, 27447–27453 (Nov 2012).

[23] Kelleher, E. J. R. and Travers, J. C., "Chirped pulse formation dynamics in ultra-long mode-locked fiber lasers," *Opt. Lett.* **39**, 1398–1401 (Mar 2014).

[24] Garbin, B., Javaloyes, J., Tissoni, G., and Barland, S., "Topological solitons as addressable phase bits in a driven laser," *Nat Commun* **6**, – (Jan. 2015).

[25] Turitsyn, S. K., Babin, S. A., Churkin, D. V., Vatnik, I. D., Nikulin, M., and Podivilov, E. V., "Random distributed feedback fibre lasers," *Physics Reports* **542**(2), 133–193 (2014).

[26] Churkin, D. V., Sugavanam, S., Vatnik, I. D., Wang, Z., Podivilov, E. V., Babin, S. A., Rao, Y., and Turitsyn, S. K., "Recent advances in fundamentals and applications of random fiber lasers," *Advances in Optics and Photonics* **7**(3), 516–569 (2015).

[27] Wu, H., Wang, Z. N., Churkin, D. V., Vatnik, I. D., Fan, M. Q., and Rao, Y. J., "Random distributed feedback raman fiber laser with polarized pumping," *Laser Physics Letters* **12**(1), 015101 (2015).

[28] Vatnik, I., Churkin, D., Podivilov, E., and Babin, S., "High-efficiency generation in a short random fiber laser," *Laser Physics Letters* **11**(7), 075101 (2014).

[29] Sugavanam, S., Yan, Z., Kamynin, V., Kurkov, A., Zhang, L., and Churkin, D., "Multiwavelength generation in a random distributed feedback fiber laser using an all fiber lyot filter," *Optics Express* **22**(3), 2839–2844 (2014).

[30] Babin, S., El-Taher, A., Harper, P., Podivilov, E., and Turitsyn, S., "Tunable random fiber laser," *Physical Review A* **84**(2), 021805 (2011).

[31] Smirnov, S. V. and Churkin, D. V., "Modeling of spectral and statistical properties of a random distributed feedback fiber laser," *Optics Express* **21**(18), 21236–21241 (2013).

[32] Churkin, D. V., Kolokolov, I. V., Podivilov, E. V., Vatnik, I. D., Nikulin, M. A., Vergeles, S. S., Terekhov, I. S., Lebedev, V. V., Falkovich, G., Babin, S. A., et al., "Wave kinetics of random fibre lasers," *Nature Communications* **2** (2015).

[33] Tarasov, N., Sugavanam, S., and Churkin, D., "Spatio-temporal generation regimes in quasi-cw raman fiber lasers," *Opt. Express* **23**, 24189–24194 (Sep 2015).

[34] Yao, B., Rao, Y., Wang, Z., Wu, Y., Zhou, J., Wu, H., Fan, M., Cao, X., Zhang, W., Chen, Y., Li, Y., D, C., S, T., and CW, W., "Graphene based widely-tunable and singly-polarized pulse generation with random fiber lasers," *Scientific reports* **5**, 18526 (2015).

[35] Picozzi, A., Garnier, J., Hansson, T., Suret, P., Randoux, S., Millot, G., and Christodoulides, D., "Optical wave turbulence: Towards a unified nonequilibrium thermodynamic formulation of statistical nonlinear optics," *Physics Reports* **542**(1), 1 – 132 (2014). Optical wave turbulence: Towards a unified nonequilibrium thermodynamic formulation of statistical nonlinear optics.

[36] Jang, J. K., Erkintalo, M., Murdoch, S. G., and Coen, S., "Ultraweak long-range interactions of solitons observed over astronomical distances," *Nat Photon* **7**, 657–663 (Aug. 2013).

[37] Jang, J. K., Erkintalo, M., Murdoch, S. G., and Coen, S., "Writing and erasing of temporal cavity solitons by direct phase modulation of the cavity driving field," *Opt. Lett.* **40**, 4755–4758 (Oct 2015).

[38] Goda, K. and Jalali, B., "Dispersive fourier transformation for fast continuous single-shot measurements," *Nature Photonics* **7**, 102–112 (Feb. 2013).

[39] Runge, A. F., Broderick, N. G., and Erkintalo, M., "Dynamics of soliton explosions in passively mode-locked fiber lasers," *JOSA B* **33**(1), 46–53 (2016).

[40] Liu, Z., Zhang, S., and Wise, F. W., "Rogue waves in a normal-dispersion fiber laser," *Optics letters* **40**(7), 1366–1369 (2015).

[41] Zhang, C., Xu, J., Chui, P., and Wong, K. K., "Parametric spectro-temporal analyzer (pasta) for real-time optical spectrum observation," *Scientific reports* **3** (2013).

[42] Walczak, P., Randoux, S., and Suret, P., "Optical rogue waves in integrable turbulence," *Physical review letters* **114**(14), 143903 (2015).